The effect of sulphonation degree on the fabrication and performance of PBI-sPPSU assymetric polymer membranes

MSc Thesis

Stijn Joachim Slaats — 1025319

MSc Biotechnology

Report number: 209BCT

Supervisor:

Dr. ir. Akbar Asadi Tashvigh

Examinor:

Dr. Elinor Scott

Contents

Abstract

This study evaluates the performance of blended polybenzimidazole (PBI)–sulfonated polyphenylsufone (sPPSU) membranes in terms of solvent permeance, salt rejection, organic micropollutant (OMP) retention, and thermal stability. The objective was to investigate the influence of sulfonation degree and crosslinking on membrane properties and separation performance.

Pure solvent permeance measurements revealed significant variability, with values ranging from 0.50 to 21.74 $L \cdot m^{-2} \cdot bar^{-1} \cdot h^{-1}$. The presence of sPPSU had a positive effect on solvent flux, with moderate sulfonation yielding the most favourable results.

Salt rejection followed an expected trend, showing a positive correlation with sulfonation degree, while the model organic micropollutant exhibited high retention across all membranes. Thermal stability analysis demonstrated that sulfonation degree did not significantly impact stability, whereas crosslinking reduced thermal resistance.

These findings indicate that sulfonation degree can serve as a tool for fine-tuning membrane properties, allowing for optimized performance based on specific separation requirements. However, further analysis is necessary to determine the precise effects on membrane structure and long-term durability.

Introduction

Nanofiltration (NF) is a pressure-driven membrane separation process characterized by pores typically ranging from 1 to 2 nm, it sits in between ultrafiltration and reverse osmosis in terms of selectivity [1], [2]. Over the past few decades, NF has found many applications in various sectors, including water treatment, food processing, and biopharmaceutical industries [3], [4]. However, in recent years there has been more interest in extending nanofiltration to organic solvent systems, often referred to as organic solvent nanofiltration (OSN). Despite its potential in industrial processes, such as pharmaceuticals and petrochemicals, OSN remains limited by the scarcity of robust, solvent-stable membrane materials with high permeability, which is one of the most important characteristics of OSN membranes [5].

Alongside industrial applications, water treatment has emerged as a critical domain for advanced membrane technologies due to the increasing pollution of organic micropollutants (OMPs) in waste-and drinking water. Current treatment methods are not always sufficient to remove these contaminants effectively, risking public health and the environment. In response, developing membrane materials that can selectively filter out OMPs while maintaining high flux has become increasingly important [6], [7]

Polymers as Membrane Materials

Polymeric materials have been crucial in membrane technology due to their versatility, straightforward fabrication procedures, and scalability [8]. These characteristics make polymers desirable for both academic research and large-scale industrial applications. In the context of OSN, many different kinds of polymers such as polyimides, polyvinyl alcohols, polymers of intrinsic microporosity (PIM) and polybenzimidazole, have been investigated for their potential to provide high chemical resistance and desirable separation characteristics [9]

Polybenzimidazole (PBI)

Among the possible polymers suitable for OSN, polybenzimidazole (PBI) stands out due to its chemical and thermal stability. It has strong resistance to oxidative, mechanical, and thermal stress, making it durable in harsh environments [5], [10]. Furthermore, the nitrogen groups in the imidazole rings allow crosslinking without major alterations to the polymer backbone, increasing chemical stability while keeping the attributes that make PBI a promising candidate for OSN [11], [12].

Despite its advantages, PBI suffers from certain drawbacks, including brittleness [13]. Additionally, PBI membranes exhibit a neutral charge near neutral pH and low hydrophobicity, which can reduce solute–membrane interactions in some applications [14].

Sulfonated Polyphenylsulfone (sPPSU)

Sulfonated polyphenylsulfone (sPPSU) has been employed in a wide range of filtration processes [15], [16] The presence of sulfonic acid groups on its backbone provides flexibility and serves as a chemical anchor for membrane functionalization, while keeping strong chemical resistance [17]. Additionally, sPPSU-based membranes have demonstrated favorable permeability in aqueous systems, making them particularly relevant for both water treatment and OSN [11], [18]

Blending and Crosslinking

To coutner act the limitations of single-polymer membranes, polymer blending has geen activly explored. This approach combines two or more polymers to create a blend membrane that possesses favorable characteristics compared to each polymer alone [19], [20], One major concern is the potential for immiscibility at the molecular level, which can lead to phase separation and lower mechanical integrity.

In parallel, crosslinking has used to increase chemical stability and fine-tune pore size [10], [11], [12], [21]. By creating covalent bonds between polymer chains, crosslinking can reduce swelling in organic solvents and tighten pores to increase selectivity which is crucial for OSN membranes.

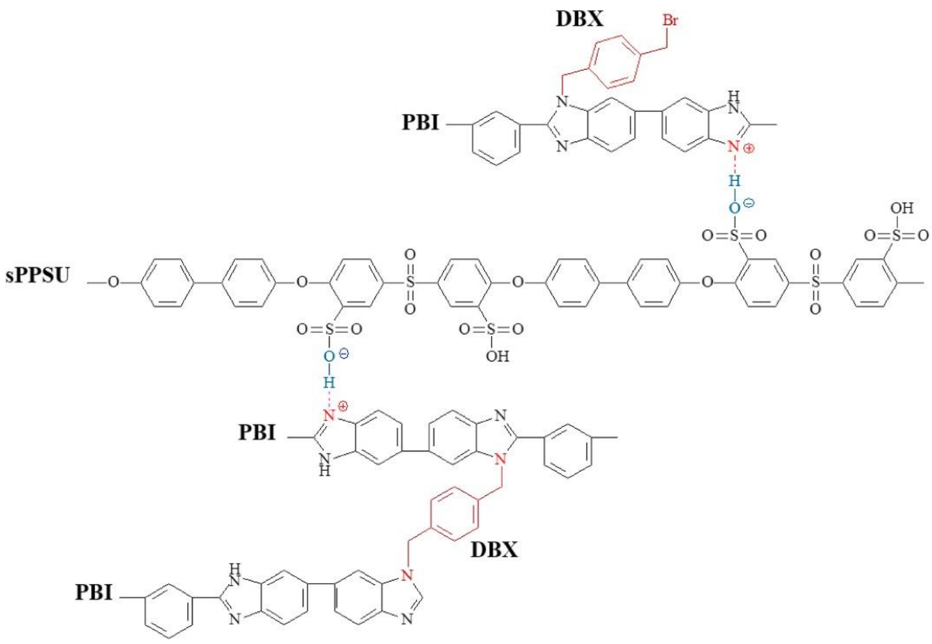

Figure 1: Binding of sPPSU and PBI with DBX as a crosslinker [22]

Research Goal

Taking into account the demand for robust and high-flux membranes to remove OMPs from water and operate effectively in diverse organic solvents, this research focuses on blended membranes made of polybenzimidazole (PBI) and sulfonated polyphenylsulfone (sPPSU). Specifically, the study aims to examine how varying the sulfonation degree in sPPSU affects membrane performance. The following key parameters will be evaluated:

Permeance in Various Organic Solvents: Assessing how changes in sulfonation degree influence solvent flux and resistance.

Rejection of Tetracycline: Using tetracycline as a model OMP to investigate selectivity.

Thermal Stability: Monitoring the effect of blending and croslinking on the maximum temperature the material is able to withstand through thermo-gravimetric analysis. (TGA)

Salt Rejection: Evaluating ion separation capabilities, which could broaden the scope of applications.

Overall, this work seeks to deepen our understanding of how functional group density, specifically sulfonation, affects membrane properties, thereby guiding the design of next-generation polymeric membranes for water treatment and solvent-based separations.

Materials

Sulfonated polyphenylsulfone (sPPSU with a sulfonation degree of 5mol%, 10mol% and 15 mol% was synthesized by BASF, Germany via direct copolymerization, using the monomer of 4,4dichlorodiphenyl sulfone (DCDPS). A polybenzimidazole (PBI, celazoles s26, Mw = 27000 g/mol) dope solution with 26wt%PBI, was acquired from PBI performance Products Inc. (USA). Nonwoven fabrics (polypropylene, Novatexx 2471) were obtained from Freudenberg group. α-α'-dibromo-p-xylene (DBZ, 97%) was acquired from Sigma-Aldrich for PBI crosslinking. N- dimethylformamide (DMF, > 99.5%, Merck) and Dimethylacetamide were used as the additive, solvent and co-solvent for membrane fabrication, respectively. For dye filtration experiments Tetracycline 98% from Sigma-Aldrich was used. Sodium sulphate (Na_2SO_4, anhydrous, Sigma-Aldrich) and magnesium chloride hexahydrate ($MgCl_2.6H_2O$, VWR Chemicals) was used for salt rejection experiments. MilliQ water, Ethanol 98%, DMF > 99%, Acetone 98%, Acetonitrile 98%. Was used for pure solvent nanofiltration experiments.

For dead-end filtration the Sterlitech HP4750 Stirred Cell was used. With a diameter of 45mm for the membrane area. Corresponding reflux magnet was used for stirring. The Dead-end filtration cell was pressurized with argon gas.

Methods

Dope solution preparation:

The sPPSU polymer was dried overnight in a vacuum oven at 80 °C to remove moisture. 0,64 g of the desired sPPSU polymer was added to 7,36 g of 26% (w/w%) PBI stock solution and 7 g DMAc. The total polymer concentration of the whole mixture was 17% (w/w%) with a sPPSU/PBI ratio of 0,25 (w/w). The desired sPPSU polymer, PBI solution and DMAc were mixed on a roller mixer until completely dissolved. After dissolving of the polymers was successful, the dope solutions were degassed for use in the casting process. The content of the dope solutions can be seen in Table 1. The names of the samples indicate the sulphonation degree of the sPPSU. M5 having 5% sulphonation, M10 having 10% sulphonation, M15 having 15% sulphonation.

Membrane code	Polymer concentration (w/w%)	Sulphonation degree of sPPSU fraction	Crosslinking agent
MPBI	17%	-	DBX

M5	17%	5%	DBX
M10	17%	10%	DBX
M15	17%	15%	DBX

Table 1: membrane composition and crosslinker

Fabrication of asymmetric PBI-sPPSU membranes

After degassing of the dope solutions, the membranes can be cast. Polypropylene nonwoven fabrics were used as a backing to cast the dope solutions. A casting knife was used to make 350 µm thick films. After casting the films were place in a water bath for 5 minutes and then transferred to a second water bath to complete the solvent exchange and phase separation over night (~8h-12h). After this the membranes were inspected for obvious holes in the selective layers. The most obvious holes were marked by a marker to avoid them during the stamping process. A 45 mm wide stamp was used to punch the membranes. After stamping the membranes were place in a container of IPA to remove any water or leftover solvent. After this the crosslinking steps of the membranes can commence.

To stabilize the polymers and enhance the tightness of the polymer membranes a crosslinking step was used. The first step of the crosslinking the membranes were emersed in acetonitrile containing 1wt% DBX at 80°C for 1h under constant stirring, this is done to make the membrane resistant enough for the second crosslinking step as suggested by [23]After this the membrane was emersed in DMF at 100 °C containing 1wt% DBX for 24h under constant stirring. After crosslinking the membrane was washed with IPA and stored in IPA until use.

Organic solvent nanofiltration experiments

The pure solvent permeance, salt retention and tetracycline retention were measured using a dead-end filtration system. The pressure was generated using a nitrogen gas cylinder connected to the dead-end filtration system with pressure gauges. Before using each membrane, the membrane was packed for 1h at 10 bar using water as the solvent. After this the following procedure was used. For each new solvent the solvent filtration is first done for 1h. After this one hour a sample was collected for 10 min and the (delta) mass was measured. Every 30 min the change in mass was calculated until the permeance was stable. At this point the measurement would be recorded as the permeance for that membrane and that solvent. For the solute experiments the same procedure was used. Additionally, the concentration of the solute was measured at every measurement time until that was deemed stable as well.

The permeance was calculated using the following formula. Using the area of the membrane (A), the sample time (t), transmembrane pressure (P) and the permeate volume(V).

$$P = \frac{V}{At\Delta p}$$

Tetracycline and salt rejection

A solution of $MgCl_2$ and $NaSO_4$ was made with a concentration of 1g/L. The filtration was first done for 1h. After that the permeance and rejection were measured every 30min until stabilized. The permeance was measured by mass differential. The concentration of the salt was measured using a conductivity meter on the permeate and retentate. The rejection was calculated using the concentration of the permeate ($C_{permeate}$) and the concentration of the feed (C_{feed}).

$$R = \left(1 - \frac{C_{permeate}}{C_{feed}}\right) \cdot 100\%$$

For the tetracycline experiment a solution of 50 ppm was made in ethanol.

Thermal gravimetric analysis.

Thermal stability and degradation of the membrane was investigated by Thermogravimetric analysis, performed between 20C and 750C with a heating rate of 5K/min under air flux of 60ml/min. as a preparation step all water was evaporated before the measurement started by heating up the sample to 100C and keeping for an hour under the same conditions. After data collection the data was translated to relative weight, using Microsoft excel. The water evaporation time was left out of the graphs.

Results and Discussion

Pure solvent nanofiltration

To investigate the influence of solvent properties on membrane performance, five different solvents were selected, representing both polar protic and apolar solvents: water, ethanol, acetone, DMF, and acetonitrile.

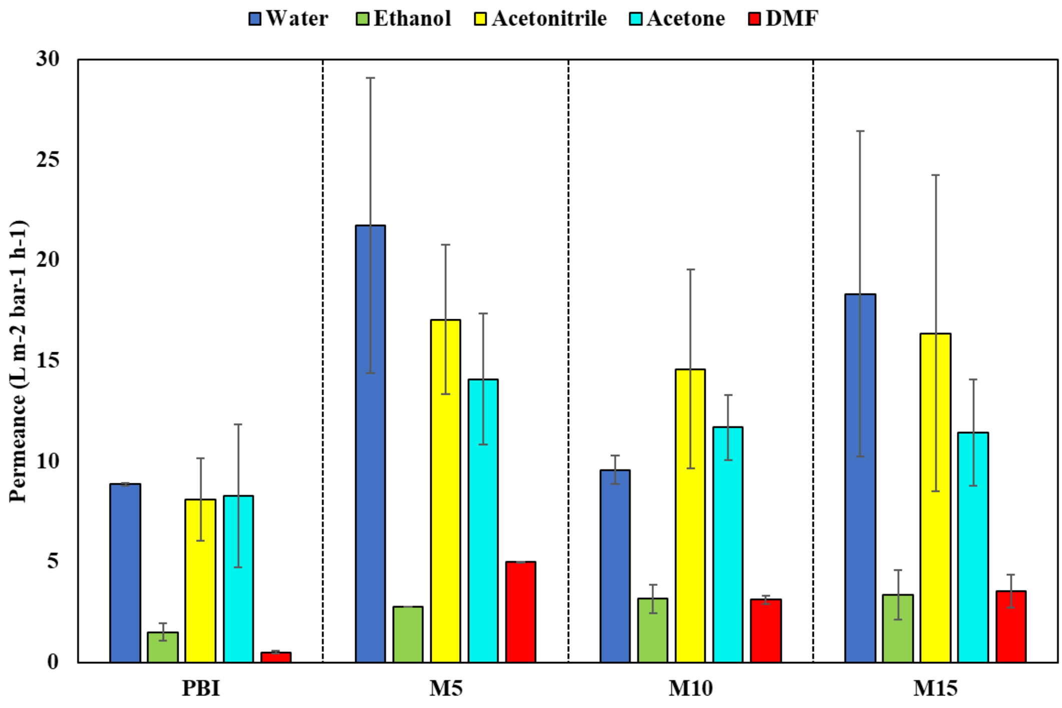

Figure 2: Pure solvent nanofiltration using 4 different solvents on membranes with different composition. PBI (no sPPSU), M5 (5 mol% sulphonation), M10 (10 mol% sulphonation), M15 (15 mol% sulphonation)

The data indicate that the physicochemical properties of the solvents have a significant impact on their permeability, and that permeability varies notably between membranes. The average permeance for the PBI membrane is 5.45 $L \cdot m^{-2} \cdot bar^{-1} \cdot h^{-1}$, the M5 membrane has the highest average permeance at 12.12 $L \cdot m^{-2} \cdot bar^{-1} \cdot h^{-1}$, the M10 membrane has an average permeance of 8.42 $L \cdot m^{-2} \cdot bar^{-1} \cdot h^{-1}$, and the M15 membrane has an average permeance of 10.60 $L \cdot m^{-2} \cdot bar^{-1} \cdot h^{-1}$. In particular, the pure PBI membrane exhibits lower permeance compared to the blend membranes, which show both higher permeance and greater variability in their results. The reduced permeance of the pure PBI membrane is likely attributed to its higher density of functional group where the crosslinker can covalently bind to, which enables tighter crosslinking, leading to smaller effective pore sizes.

Conversely, the addition of sPPSU to the blend membranes decreases the abundance of functional groups available for crosslinking, resulting in a lower degree of crosslinking and a more open membrane structure with larger effective pore sizes. This structural modification enhances solvent transport, contributing to the higher permeance observed in the blend membranes.

In addition to introducing a less compact pore structure, [24] found that the incorporation of sPPSU increased the hydrophilicity of the membranes, further contributing to the increased permeance of polar solvents.

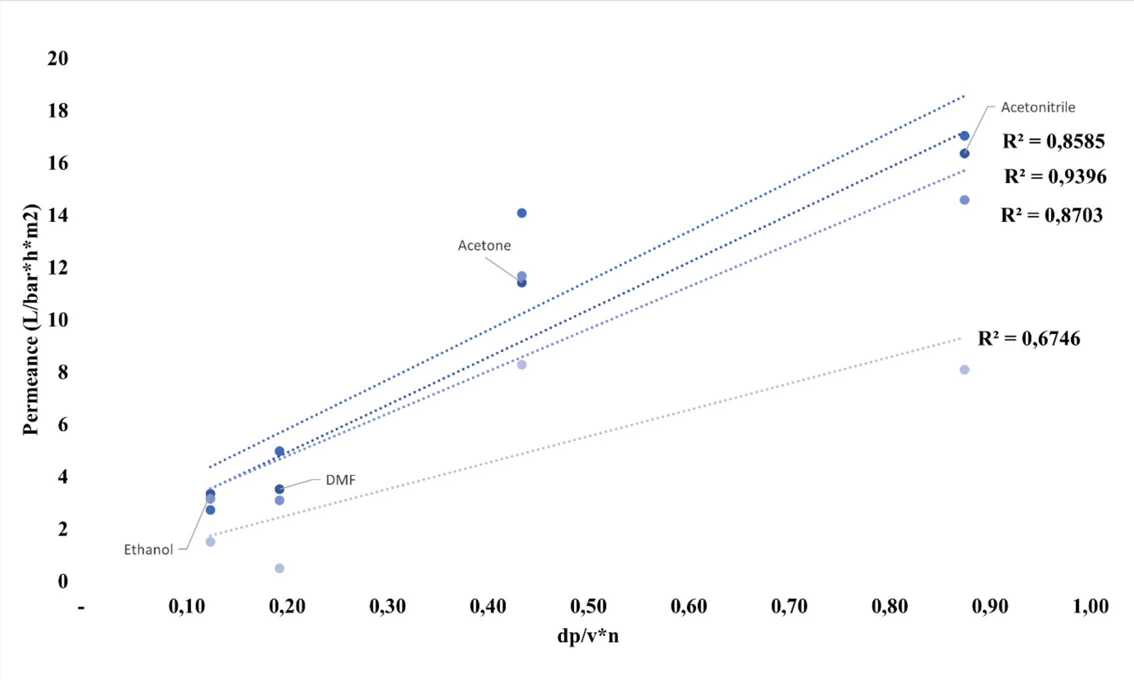

Figure 3: Graph of permeance plotted against $\frac{\delta_p}{MV\eta}$ as a way of showing the effect of the physio chemical properties of solvents on the permeance.

Furthermore, solvent permeance generally follows the trend water>acetonitrile > acetone > DMF > ethanol. This suggests that solvent transport is influenced by key physiochemical properties such as the solubility parameter, viscosity, and molar volume. Figure 3 further supports this observation, showing a correlation between membrane permeance and the parameter ΔP / (MV × η), where ΔP is the solubility parameter, MV is the molar volume, and η is the solvent viscosity. This correlation indicates that, for the blend membranes, these three properties—molar volume, solubility parameter, and viscosity—are the dominant factors governing solvent permeance. Which is also what [25] found for similar membranes.

The high standard deviation observed in the pure solvent permeance measurements suggests that the production process of these membranes may have been too variable, leading to inconsistencies in membrane structure and performance. Variations in polymer mixing, casting conditions, or crosslinking efficiency could have contributed to differences in pore distribution and membrane homogeneity, resulting in fluctuations in permeance. A more standardized and controlled production process would likely reduce these variations, leading to a more consistent membrane structure and a lower spread in permeance values across different samples.

Salt retention

To investigate the influence of membrane charge and pore structure on salt rejection, two different salts were tested: Na_2SO_4 and $MgCl_2$. These salts were chosen to evaluate the effect of ion valency on rejection and to infer the membrane's charge characteristics. A higher rejection of Na_2SO_4 would indicate a more negatively charged membrane, as the negatively charged SO_4^{2-} ions would be strongly repelled due to Donnan exclusion. Conversely, a higher rejection of $MgCl_2$ would suggest a more positively charged membrane, as the divalent Mg^{2+} ions would be repelled.

For Na_2SO_4 rejection, the PBI membrane shows the highest retention (0.71), while M5 has the lowest (0.14). The M10 and M15 membranes exhibit intermediate values (0.30 and 0.28, respectively). In terms of permeance, M5 has the highest value (15.17 $L \cdot m^{-2} \cdot bar^{-1} \cdot h^{-1}$), while PBI has the lowest (6.29 $L \cdot m^{-2} \cdot bar^{-1} \cdot h^{-1}$), with M10 and M15 falling in between (9.60 $L \cdot m^{-2} \cdot bar^{-1} \cdot h^{-1}$ and 10.72 $L \cdot m^{-2} \cdot bar^{-1} \cdot h^{-1}$, respectively).

For $MgCl_2$ rejection, PBI again has the highest retention (0.97), while M5 has the lowest (0.62), and M10 and M15 fall in between (0.71 and 0.80, respectively). In terms of permeance, M5 exhibits the highest value (12.71 $L \cdot m^{-2} \cdot bar^{-1} \cdot h^{-1}$), while PBI has the lowest (7.07 $L \cdot m^{-2} \cdot bar^{-1} \cdot h^{-1}$), with M10 and M15 showing values of 8.80 $L \cdot m^{-2} \cdot bar^{-1} \cdot h^{-1}$ and 8.19 $L \cdot m^{-2} \cdot bar^{-1} \cdot h^{-1}$, respectively.

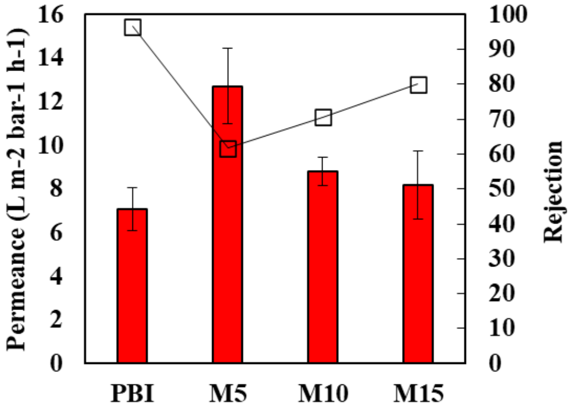

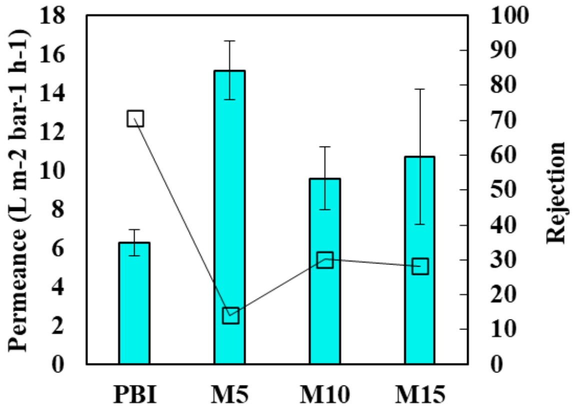

Figure 4A: Permeance and retention of Na2SO4 solution of crosslinked sPPSU-PBI membranes. PBI (no sPPSU), M5 (5mol% sulphonation), M10 (10mol% sulphonation), M15 (15mol% sulphonation)

Figure 4B: Permeance and retention of MgCl2 solution of crosslinked sPPSU-PBI membranes PBI (no sPPSU), M5 (5mol% sulphonation), M10 (10mol% sulphonation), M15 (15mol% sulphonation)

When comparing the rejection trends in Figures 4a and 4b, it becomes evident that all membranes exhibited a higher rejection of Na_2SO_4 compared to $MgCl_2$. This strongly suggests that the membranes are negatively charged, as the SO_4^{2-} ions experience stronger electrostatic repulsion, leading to higher rejection. This trend aligns with the Donnan exclusion principle, which states that charged membranes preferentially repel co-ions of the same charge, further enhancing the rejection of divalent anions like SO_4^{2-} [26].

Additionally, the salt rejection results support previous observations regarding pure solvent permeance, particularly in relation to membrane composition and pore size. The M5 membrane, which has the lowest sulfonation degree and consequently a lower density of functional groups, was found to have the largest effective pore size. This is reflected in its lowest rejection for both Na_2SO_4 and $MgCl_2$ compared to the other membranes. The larger pore size facilitates ion transport, reducing overall salt rejection. In contrast, the PBI membrane, known for its small pore size due to its higher degree of crosslinking, demonstrated relatively high salt rejection, suggesting that steric hindrance also contributes to separation performance.

Further insight into the role of functional group density is provided by the differences in salt rejection between the M10 and M15 membranes. The higher rejection of $MgCl_2$ in M10 and M15 can be attributed to greater steric hindrance, as the increased presence of functional groups leads to a denser membrane structure, making ion passage more difficult. At the same time, the higher rejection of Na_2SO_4 in these membranes can be linked not only to steric hindrance but also to an enhanced charge effect. A higher sulfonation degree introduces more negative charge, which strengthens electrostatic repulsion against sulfate ions, leading to even higher rejection.

Overall, these results demonstrate that both charge exclusion and steric hindrance contribute to salt rejection, but charge exclusion likely plays the more dominant role. This conclusion is supported by the consistently higher rejection of Na_2SO_4 across all membranes, indicating that electrostatic interactions govern separation performance more significantly than steric effects. Although steric hindrance is relevant, particularly in membranes with a high density of functional groups, the strong correlation between membrane charge and sulphate rejection reinforces the idea that electrostatic interactions are the primary mechanism in NF membrane performance [27]

Tetracycline retention

Tetracycline was used as a model compound to evaluate the ability of these membranes to retain organic micropollutants (OMPs) and to estimate a lower bound for the molecular weight cut-off (MWCO). The wavelength at which tetracycline exhibits the highest absorbance is 356 nm, which serves as a key reference point in the UV-Vis spectra.

Figures 5A–5D present the absorbance spectra of both the retentate (red line) and permeate (cyan line) for the tested membranes. In Figure 5A, the retentate measurement shows a fingerprint region below 190 nm, a peak at approximately 280 nm, and a prominent peak at 356 nm. The corresponding permeate measurement exhibits no clearly visible peaks beyond the fingerprint region, indicating effective tetracycline retention. A similar trend is observed in Figure 5B, where the retentate spectrum again displays peaks at 280 nm and 356 nm, while the permeate spectrum lacks peaks beyond the fingerprint region. In Figure 5C, the retentate measurement follows the same pattern, with peaks at 280 nm and 356 nm, whereas the permeate measurement deviates slightly by displaying a peak at 280 nm, likely due to contamination. Finally, in Figure 5D, the retentate measurement retains peaks at 280 nm and 356 nm, while the permeate spectrum shows no peaks at all.

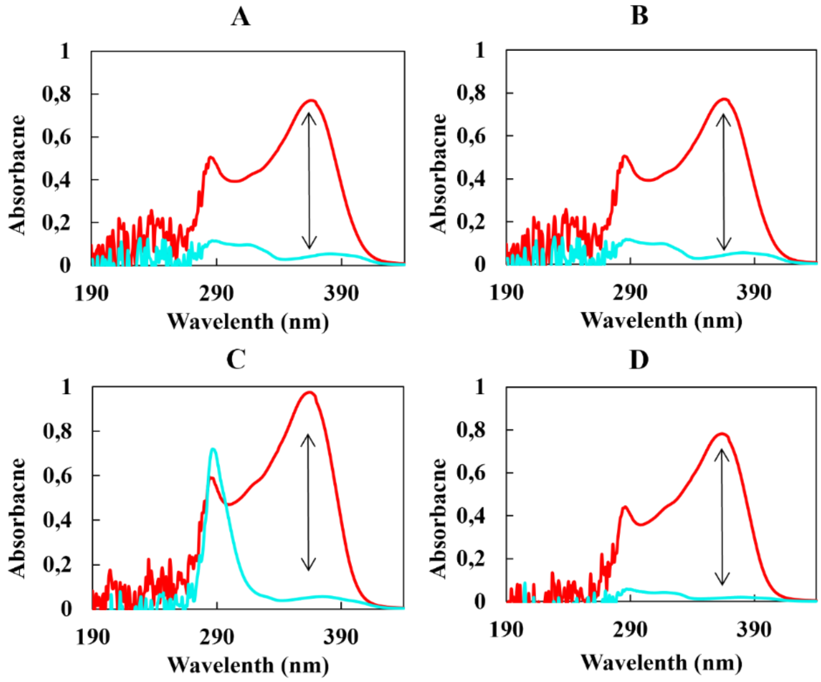

Figure 5: Tetracycline retention of four sPPSU-PBI membranes with increasing sulphonation degree of the sPPSU fraction. Absorbance of the retentate is shown in red, absorbance of the permeate is shown in cyan. Different graphs are for the different membranes that were fabricated. A: PBI (no sPPSU), B:M5 (sPPSU 5mol% sulphonation), C:M10 (sPPSU 10mol% sulphonation), D:M15 (sPPSU 15mol% sulphonation)

The absence of a 356 nm peak in all permeate spectra confirms the high retention of tetracycline across all membranes. The only irregularity is the 280 nm peak in the permeate measurement of Figure 5C, which is likely an artifact due to contamination rather than a sign of tetracycline passage.

These results indicate that tetracycline retention is independent of sPPSU content and the sulfonation degree of the sPPSU fraction. This aligns with findings from [11], which reported high rejection of Rose Bengal using a similar blended polymer membrane and crosslinking technique. Since Rose Bengal has a molecular weight approximately twice that of tetracycline, and these membranes show similar retention behaviour, it can be concluded that the MWCO is lower than 444 g/mol.

Furthermore, these findings demonstrate a higher tetracycline retention than reported in [5] . It was previously hypothesized that a stronger solvent during the crosslinking step would induce more polymer rearrangement and enhance interlinking, ultimately improving tetracycline retention. The present results confirm this hypothesis, as the membranes in this study—where a stronger solvent (DMF) was used instead of acetonitrile—exhibited higher tetracycline retention.

Thermal stability

Thermogravimetric analysis (TGA) is a crucial technique in membrane characterization as it provides insights into the thermal stability and degradation behaviour of polymeric membranes. By measuring weight loss as a function of temperature, TGA helps assess the effect of crosslinking, polymer composition, and functional group modifications on membrane stability and performance.

Figure 6 depicts the relative weight loss of the membranes as temperature increases. A weight decrease occurs around 220°C for all membranes, followed by a stabilization phase until another significant weight loss at approximately 450°C, after which the weight decreases linearly. This degradation profile differs from pure PBI membranes ([reference]), suggesting that the sulfonation process and blending affect the thermal behaviour. However, the similar weight-loss patterns across all membranes indicate that the degree of sulfonation does not significantly impact thermal stability.

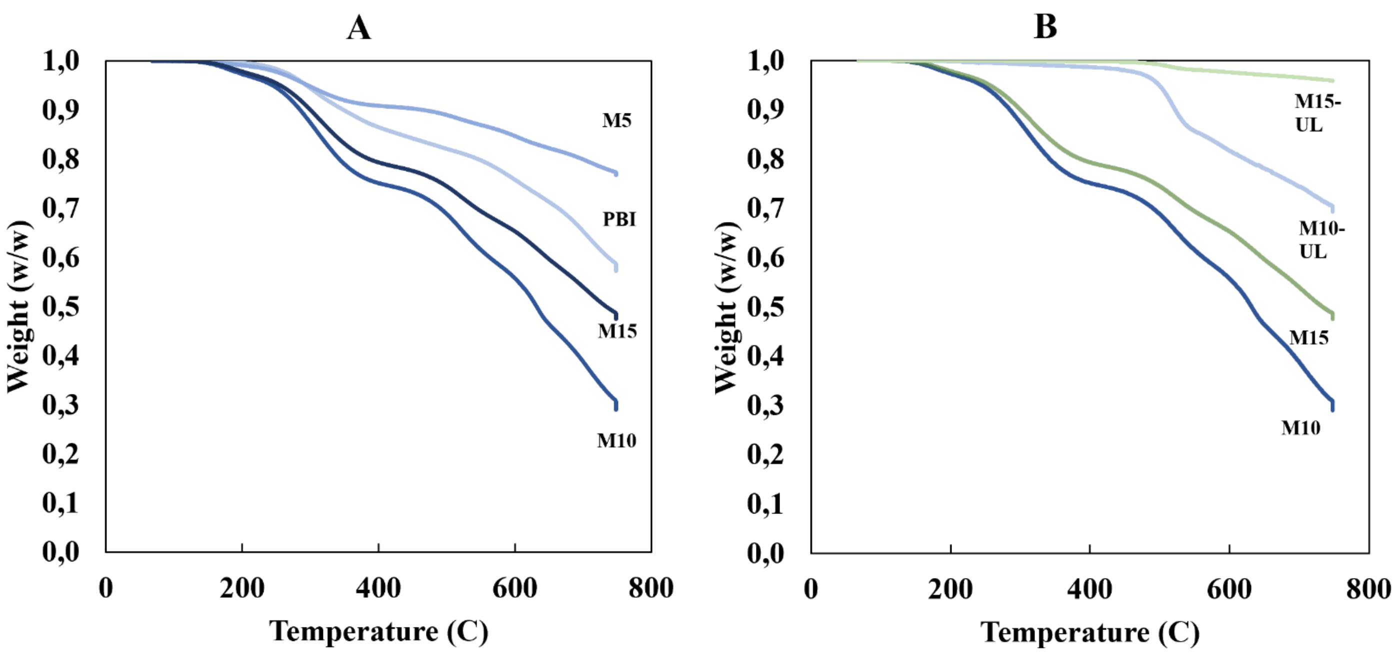

Figure 6A: Thermal gravimetric analysis of sPPSU-PBI membranes. The graph shows the relative weight loss at a temperature between 25C and 750C. All crosslinked membranes were tested, PBI, M5, M10 and M15. From shape of the graph the thermal stability can be concluded.

Figure 6B: Thermal gravimetric analysis of crosslinked and uncross linked sPPSU-PBI membranes. The membranes tested was M15 and M10 and the non-crosslinked versions of the membrane M15-UL and M10-UL.

The graph also illustrates the thermal stability of the membranes before and after crosslinking. The green line represents an M15 membrane, while the blue line represents an M10 membrane. A darker-coloured line indicates the crosslinked membrane. The crosslinked membranes exhibit weight loss around 200°C, and both follow a similar degradation pattern, suggesting that their composition is comparable. However, the crosslinked membranes display a more irregular weight-loss curve, indicating possible structural changes due to the crosslinking process. In contrast, the non-crosslinked membranes begin degrading around 500°C, with similar thermal behaviour across different sulfonation degrees.

These results suggest that one of the key advantages of PBI membranes—their thermal stability—is compromised after the crosslinking step. The initial weight loss at 200°C corresponds to the degradation of crosslinking bonds, confirming that thermal stability is strongly influenced by the crosslinking process rather than the sulfonation degree. However, the thermal stability is above 200°C which allows these membranes to be used in an industrial setting [28].

Conclusion and recommendation

The analysis of pure solvent permeance provided insight into the structural properties of the membranes. The PBI membrane exhibited the narrowest range of permeance values, spanning from 0.50 to 8.86 $L \cdot m^{-2} \cdot bar^{-1} \cdot h^{-1}$, indicating lower overall permeability. The M5 membrane showed the widest range, with permeance values between 2.74 and 21.74 $L \cdot m^{-2} \cdot bar^{-1} \cdot h^{-1}$, reflecting significant variability. The M10 membrane had a range of 3.11 to 14.59 $L \cdot m^{-2} \cdot bar^{-1} \cdot h^{-1}$, while the M15 membrane exhibited values between 3.36 and 18.33 $L \cdot m^{-2} \cdot bar^{-1} \cdot h^{-1}$, both showing higher permeance than PBI but with slightly less variability than M5.

In terms of salt rejection, all membranes exhibited higher rejection of Na_2SO_4 compared to $MgCl_2$, confirming that they are negatively charged. Although steric effects contributed, charge exclusion was identified as the dominant mechanism governing salt retention. Sulphonation degree does influence the salt rejection of these polymeric membranes, with both salt species having higher rejection with higher sulphonation degree.

For tetracycline rejection, results demonstrated consistently high retention across all membranes, independent of sPPSU content or sulfonation degree. The absence of a 356 nm peak in the permeate spectra confirmed that tetracycline was effectively retained by all membranes.

Thermal stability assessments using TGA showed that sulfonation degree does not significantly impact thermal stability. However, crosslinking significantly altered the thermal behavior.

To improve the reliability and performance of these membranes, several steps should be taken. First, the production process should be standardized to reduce the high variation observed in pure solvent permeance. Inconsistencies in membrane fabrication, such as variations in polymer mixing, casting conditions, and crosslinking efficiency, likely contributed to differences in pore structure and polymer distribution. A more controlled and precise manufacturing process would help minimize these discrepancies, leading to greater reproducibility and consistency in membrane performance.

Additionally, further characterization is necessary to better understand the factors contributing to the observed variation in pure solvent permeance. One approach is to perform water contact angle measurements, which would provide insights into membrane hydrophilicity and surface energy, both of which influence solvent-membrane interactions and permeability. Furthermore, electron microscopy techniques, such as SEM, could be used to analyse surface morphology and pore structure, helping to identify any inhomogeneities that may contribute to the differences in permeance. Beyond structural characterization, long-term stability testing should be conducted to assess the mechanical robustness, and chemical durability of the membranes under extended operational conditions. Understanding how these membranes perform over time would be essential for evaluating their practical applicability and reliability in real-world filtration processes.

By implementing these recommendations, the variability in membrane performance can be better understood and mitigated, ultimately leading to more consistent and reliable membrane properties suited for a range of separation applications.

Bibliography

[1] P. Vandezande, L. E. M. Gevers, and I. F. J. Vankelecom, “Solvent resistant nanofiltration: Separating on a molecular level,” *Chem Soc Rev*, vol. 37, no. 2, pp. 365–405, Jan. 2008, doi: 10.1039/B610848M.

[2] A. W. Mohammad, Y. H. Teow, W. L. Ang, Y. T. Chung, D. L. Oatley-Radcliffe, and N. Hilal, “Nanofiltration membranes review: Recent advances and future prospects,” *Desalination*, vol. 356, pp. 226–254, Jan. 2015, doi: 10.1016/J.DESAL.2014.10.043.

[3] M. Sadrzadeh, J. Hajinasiri, S. Bhattacharjee, and D. Pernitsky, “Nanofiltration of oil sands boiler feed water: Effect of pH on water flux and organic and dissolved solid rejection,” *Sep Purif Technol*, vol. 141, pp. 339–353, Feb. 2015, doi: 10.1016/J.SEPPUR.2014.12.011.

[4] Z. Tang *et al.*, “Design and fabrication of electrospun polyethersulfone nanofibrous scaffold for high-flux nanofiltration membranes,” *J Polym Sci B Polym Phys*, vol. 47, no. 22, pp. 2288–2300, Nov. 2009, doi: 10.1002/POLB.21831.

[5] A. Asadi Tashvigh, L. Luo, T. S. Chung, M. Weber, and C. Maletzko, “Performance enhancement in organic solvent nanofiltration by double crosslinking technique using sulfonated polyphenylsulfone (sPPSU) and polybenzimidazole (PBI),” *J Memb Sci*, vol. 551, pp. 204–213, Apr. 2018, doi: 10.1016/J.MEMSCI.2018.01.047.

[6] K. V. Plakas, A. J. Karabelas, T. Wintgens, and T. Melin, “A study of selected herbicides retention by nanofiltration membranes-The role of organic fouling,” *J Memb Sci*, vol. 284, no. 1–2, pp. 291–300, Nov. 2006, doi: 10.1016/J.MEMSCI.2006.07.054.

[7] A. Huber, M. Bach, and H. G. Frede, “Pollution of surface waters with pesticides in Germany: Modeling non-point source inputs,” *Agric Ecosyst Environ*, vol. 80, no. 3, pp. 191–204, Sep. 2000, doi: 10.1016/S0167-8809(00)00145-6.

[8] W. F. Yong and H. Zhang, “Recent advances in polymer blend membranes for gas separation and pervaporation,” *Prog Mater Sci*, vol. 116, p. 100713, Feb. 2021, doi: 10.1016/J.PMATSCI.2020.100713.

[9] W. F. Yong and H. Zhang, “Recent advances in polymer blend membranes for gas separation and pervaporation,” *Prog Mater Sci*, vol. 116, Feb. 2021, doi: 10.1016/J.PMATSCI.2020.100713.

[10] S. S. Beshahwored, Y. H. Huang, Z. G. Abdi, C. C. Hu, and T. S. Chung, “Polybenzimidazole (PBI) membranes cross-linked with various cross-linkers and impregnated with 4-sulfocalix [4]arene (SCA4) for organic solvent nanofiltration (OSN),” *J Memb Sci*, vol. 663, p. 121039, Dec. 2022, doi: 10.1016/J.MEMSCI.2022.121039.

[11] M. H. Davood Abadi Farahani and T. S. Chung, “A novel crosslinking technique towards the fabrication of high-flux polybenzimidazole (PBI) membranes for organic solvent nanofiltration (OSN),” *Sep Purif Technol*, vol. 209, pp. 182–192, Jan. 2019, doi: 10.1016/J.SEPPUR.2018.07.026.

[12] I. B. Valtcheva, P. Marchetti, and A. G. Livingston, “Crosslinked polybenzimidazole membranes for organic solvent nanofiltration (OSN): Analysis of crosslinking reaction mechanism and effects of reaction parameters,” *J Memb Sci*, vol. 493, pp. 568–579, Nov. 2015, doi: 10.1016/J.MEMSCI.2015.06.056.

[13] T.-S. Chung, “A critical review of polybenzimidazoles: Historical development and future R&D,” 1997. Accessed: Jan. 13, 2025. [Online]. Available: http://scholarbank.nus.edu.sg/handle/10635/91829

[14] R. Hausman, B. Digman, I. C. Escobar, M. Coleman, and T. S. Chung, “Functionalization of polybenzimidizole membranes to impart negative charge and hydrophilicity,” *J Memb Sci*, vol. 363, no. 1–2, pp. 195–203, Nov. 2010, doi: 10.1016/J.MEMSCI.2010.07.027.

[15] Y. Liu *et al.*, “Synthesis of sulfonated polyphenylsulfone as candidates for antifouling ultrafiltration membrane,” *Sep Purif Technol*, vol. 98, pp. 298–307, Sep. 2012, doi: 10.1016/J.SEPPUR.2012.06.031.

[16] Y. Feng *et al.*, “Rheology and phase inversion behavior of polyphenylenesulfone (PPSU) and sulfonated PPSU for membrane formation,” *Polymer (Guildf)*, vol. 99, pp. 72–82, Sep. 2016, doi: 10.1016/J.POLYMER.2016.06.064.

[17] Y. Feng, M. Weber, C. Maletzko, and T. S. Chung, “Fabrication of organic solvent nanofiltration membranes via facile bioinspired one-step modification,” *Chem Eng Sci*, vol. 198, pp. 74–84, Apr. 2019, doi: 10.1016/J.CES.2019.01.008.

[18] G. Han *et al.*, “High performance thin-film composite membranes with mesh-reinforced hydrophilic sulfonated polyphenylenesulfone (sPPSU) substrates for osmotically driven processes,” *J Memb Sci*, vol. 502, pp. 84–93, Mar. 2016, doi: 10.1016/J.MEMSCI.2015.12.023.

[19] J. Yang, Y. Wang, G. Yang, and S. Zhan, “New anhydrous proton exchange membranes based on fluoropolymers blend imidazolium poly (aromatic ether ketone)s for high temperature polymer electrolyte fuel cells,” *Int J Hydrogen Energy*, vol. 43, no. 17, pp. 8464–8473, Apr. 2018, doi: 10.1016/J.IJHYDENE.2018.03.128.

[20] H. B. Hopfenberg and D. R. Paul, “Transport Phenomena in Polymer Blends,” *Polymer Blends*, pp. 445–489, Jan. 1978, doi: 10.1016/B978-0-12-546801-5.50016-5.

[21] T. O. McDonald *et al.*, “Using intermolecular interactions to crosslink PIM-1 and modify its gas sorption properties,” *J Mater Chem A Mater*, vol. 3, no. 9, pp. 4855–4864, Feb. 2015, doi: 10.1039/C4TA06070A.

[22] A. Naderi, A. Asadi Tashvigh, T. S. Chung, M. Weber, and C. Maletzko, “Molecular design of double crosslinked sulfonated polyphenylsulfone /polybenzimidazole blend membranes for an efficient hydrogen purification,” *J Memb Sci*, vol. 563, pp. 726–733, Oct. 2018, doi: 10.1016/J.MEMSCI.2018.06.033.

[23] I. B. Valtcheva, S. C. Kumbharkar, J. F. Kim, Y. Bhole, and A. G. Livingston, “Beyond polyimide: Crosslinked polybenzimidazole membranes for organic solvent nanofiltration (OSN) in harsh environments,” *J Memb Sci*, vol. 457, pp. 62–72, May 2014, doi: 10.1016/J.MEMSCI.2013.12.069.

[24] Y. Feng, M. Weber, C. Maletzko, and T. S. Chung, “Facile fabrication of sulfonated polyphenylenesulfone (sPPSU) membranes with high separation performance for organic solvent nanofiltration,” *J Memb Sci*, vol. 549, pp. 550–558, Mar. 2018, doi: 10.1016/J.MEMSCI.2017.12.048.

[25] S. S. Beshahwored, M. Weber, C. C. Hu, J. Y. Lai, and T. S. Chung, “Effects of sulfonation degree on compatibility and separation performance of polybenzimidazole

(PBI)-sulfonated polyphenylenesulfone (sPPSU) blend membranes," *J Memb Sci*, vol. 683, p. 121849, Oct. 2023, doi: 10.1016/J.MEMSCI.2023.121849.

[26] H. Zhu, A. Szymczyk, and B. Balannec, "On the salt rejection properties of nanofiltration polyamide membranes formed by interfacial polymerization," *J Memb Sci*, vol. 379, no. 1–2, pp. 215–223, Sep. 2011, doi: 10.1016/J.MEMSCI.2011.05.062.

[27] S. Yu, M. Liu, M. Ma, M. Qi, Z. Lü, and C. Gao, "Impacts of membrane properties on reactive dye removal from dye/salt mixtures by asymmetric cellulose acetate and composite polyamide nanofiltration membranes," *J Memb Sci*, vol. 350, no. 1–2, pp. 83–91, Mar. 2010, doi: 10.1016/J.MEMSCI.2009.12.014.

[28] A. Asadi Tashvigh and T. S. Chung, "Robust polybenzimidazole (PBI) hollow fiber membranes for organic solvent nanofiltration," *J Memb Sci*, vol. 572, pp. 580–587, Feb. 2019, doi: 10.1016/J.MEMSCI.2018.11.048.